DENSITY FUNCTIONAL THEORY STUDY OF GEOMETRICAL AND ELECTRON STRUCTURES OF $Al_{18}Ti$ ALUMINUM CLUSTERS AS WELL AS THEIR CATALYTIC ACTIVITY TOWARD THE CO OXIDATION

Pham Thi Thanh Hoa[1,2], Ngo Tuan Cuong[1,2,*]

[1]*Faculty of Chemistry, Hanoi National University of Education, Vietnam*

[2]*Center for Computational Science, Hanoi National University of Education, Vietnam*

Abstract: *The B3LYP functional in conjunction with 6-311+G(d) basis set was employed to optimize geometrical structures, followed by frequency calculations of the Al_{19}^+ and $Al_{18}Ti$ clusters, converging to the double icosahedron structure, and the Ti places at the top apex of the double icosahedron in the case of $Al_{18}Ti$ cluster. The changes in the electron structure of the clusters have been determined; accordingly, there is energy level splitting of the 1P, 1D, 1F, 2P, and 2D shell orbitals and the appearance of 3d orbitals of the Ti in the electron configurations. The catalytic ability of the $Al_{18}Ti$ cluster for the CO and O_2 reaction has been investigated initially; thus, the Ti atom plays a central role in binding to CO and O_2, weakening both the O=O and C≡O bonds and facilitating the formation of CO_2.*

Keywords: *Al_{19}^+, $Al_{18}Ti$ clusters, density functional theory (DFT), time-dependent density functional theory (TD-DFT), CO oxidation*

1. INTRODUCTION

In recent years, theoretical and experimental studies on clusters, especially metal clusters, to investigate their geometrical, electronic, optical, and magnetic properties have been developing rapidly (Knickelbein, 2001; Reinhard & Suraud, 2004; Baletto & Ferrando, 2005; Wang et al., 2010; Li et al., 2011). Clusters can be composed of identical or two or more different types of atoms. The physical and chemical properties of clusters are not only significantly different from those of discrete molecules or large-sized materials, but also change significantly when the size and charge of the clusters change. Therefore, studying the correlation between the structure of clusters and the size and charge of clusters is a prerequisite for understanding their special physical and chemical properties.

Aluminum (Al) clusters have been extensively studied, both for the sake of basic science and for a wide range of technological applications (Jia et al., 2002; Roach et al., 2009). Researchers have used various experimental methods to fabricate Al clusters. In addition, studies on geometric structures and electronic properties have also been conducted simultaneously using various theoretical calculation methods. Two typical structures of aluminum clusters, including Al_{13}^- and Al_{19}^+ clusters, are shown in Figure 1. Relative stability has been evaluated for many types of aluminium clusters of different sizes (Chuang et al., 2006). Rao *et al.* have studied the stable geometries of neutral, cationic, and anionic Al clusters containing up to 15 atoms. The electronic structures, binding energies, relative stability, fragmentation channels, and ionization energies have been studied subsequently (Rao & Jena, 1999).

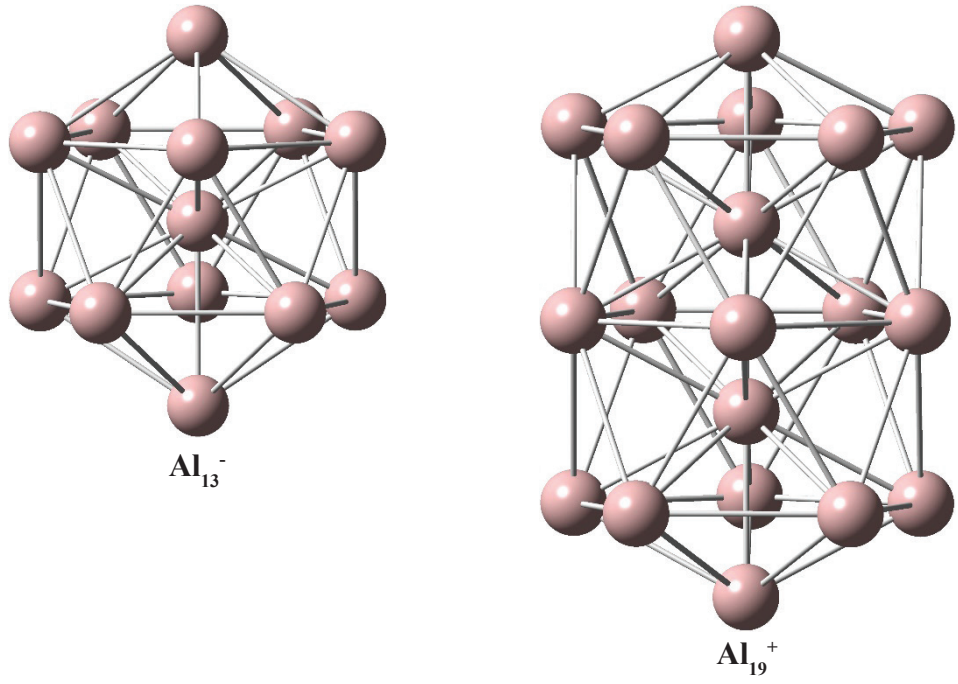

Figure 1. Geometrical structure of anionic cluster Al_{13}^- and cationic cluster Al_{19}^+

Clusters containing several atoms have molecular properties with discrete electron energy levels. When interacting with photons, they undergo energy level transitions, and as a result, absorption and emission processes occur. Therefore, they can emit radiation in the ultraviolet-visible region. Clusters containing aluminum have enormous potential for applications in materials science at the nanoscale, or even sub-nanometer scale.

Doping transition metal atoms into aluminium clusters has been identified as an effective method to improve their stability, chemical reactivity, and electronic properties. Many doped Al atomic clusters have been studied by theoretical or experimental methods, such as $Al_{12}X$ (X = B, Al, Ga, C, Si, Ge) (Charkin et al., 2002), $Al_nSi_m^{0/+}$ (with n = 3–16 and m = 1, 2) (Nguyen Minh Tam et al., 2019), and Al_nM (M = Cr, Mn, Fe, Co, Ni; n = 1–7, 12) (Wang et al., 2009). The chemical reactivity of Al atomic clusters can be significantly tuned by doping certain atoms (Varano et al., 2010; Sengupta et al., 2016; Wang & Li, 2020; Chen et al., 2021). In addition, some bimetallic clusters or ions, such as MAl_4^- (M = Li, Na, Cu) and XAl_3^- (X = Si, Ge, Sn, Pb), exhibit aromatic characteristics (Li et al., 2001, *Science*, p. 859; Li et al., 2001, *Angewandte Chemie*, p. 1919). This extends the concept of aromaticity to the field of metal clusters.

Transition metal elements are characterized by a partially filled d-shell. The magnetic and strength properties of aluminium clusters can be tuned by doping transition metal elements (Ge et al., 2013; Li et al., 2016; Yang et al., 2016; Fan et al., 2017). For example, Cr can be useful in improving the stability, magnetic, and chemical properties of Al-based materials. In particular, Al-Cr alloy coatings have good hardness and corrosion resistance, which are mainly known as aircraft structural components. For example, Al alloys with 5% Cr were successfully produced by Esquivel et al. (2017), showing significantly higher corrosion resistance and hardness.

However, the geometrical structures of Al clusters with sizes ranging from Al_{15} and larger doped with transition metals, as well as their correlation with chemical and physical properties, has not been clarified. Specifically, we found that studies on the aluminum clusters doped with transition metals $Al_{18}M$, with M being a transition metal, are still limited. The influence of doping elements on their electron structure, geometrical structure, and catalytic activity is still unclear and is an issue that needs to be studied. The dissociation process of these $Al_{18}M$ clusters into smaller atoms and clusters is also an issue that needs to be clarified.

2. METHODS OF CALCULATION

In order to study the Al_{19}^+ and $Al_{18}Ti$ clusters, we use the methods of density functional theory (DFT) and time-dependent density functional theory (TD-DFT) which are implemented in the Gaussian 09 software (Frisch et al., 2009; Hohenberg & Kohn, 1964).

Firstly, the geometries of the double icosahedron the Al_{19} cluster have been optimized using the B3LYP/6-311+G(d) functional and basis set (McLean & Chandler, 1980; Raghavachari, 1980; Becke, 1993; Perdew, 1996). These calculations are followed by frequency calculations to confirm that the stationary structures are minima. From the optimized coordinates of the Al_{19} cluster, we used quantum chemical calculation methods to calculate the geometrical structural characteristics of the Al_{19}^+ and $Al_{18}Ti$ clusters. The relative energy between the isomers was also calculated to confirm the most stable cluster. The obtained stable structures do not have negative vibrational frequencies. The stable geometrical structures and the structural and energetic parameters of the studied clusters are presented in the following subsections.

3. RESULTS AND DISCUSSION

3.1. Geometries of the Al_{19}^+ and $Al_{18}Ti$ clusters (M = Sc - Co)

3.1.1. Cluster Al_{19}^+

The geometrical structure of the Al_{19}^+ cluster is represented in Figure 2, which adopts a double icosahedron.

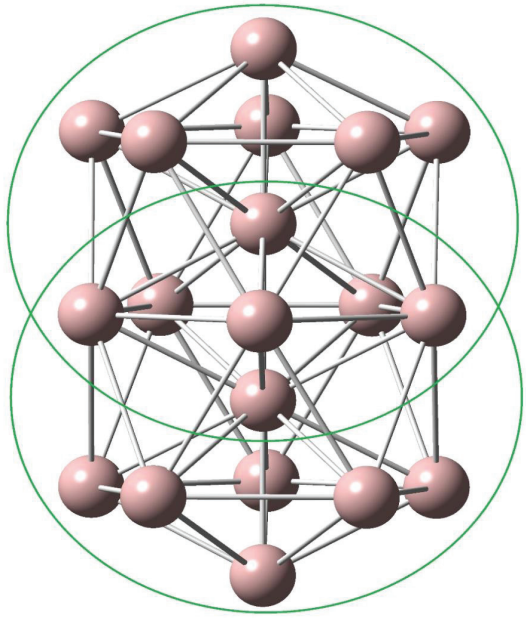

Figure 2. Geometrical structure of the Al_{19}^+ cluster

3.1.2. Geometrical structures of the $Al_{18}Ti$ cluster

From the optimized geometrical structure of the Al_{19} cluster, we replaced an Al atom with a Ti atom at four possible positions, forming the $Al_{18}Ti$ cluster with different spins. After performing the geometry optimization calculation, we obtained four convergent structures for the $Al_{18}Ti$ cluster with spin multiplicities of 1 and 3. Of the four stable structures, the one with the Ti atom at the vertex position of the double icosahedral with a spin multiplicity of 3 is the most stable structure, as shown in Figure 3.

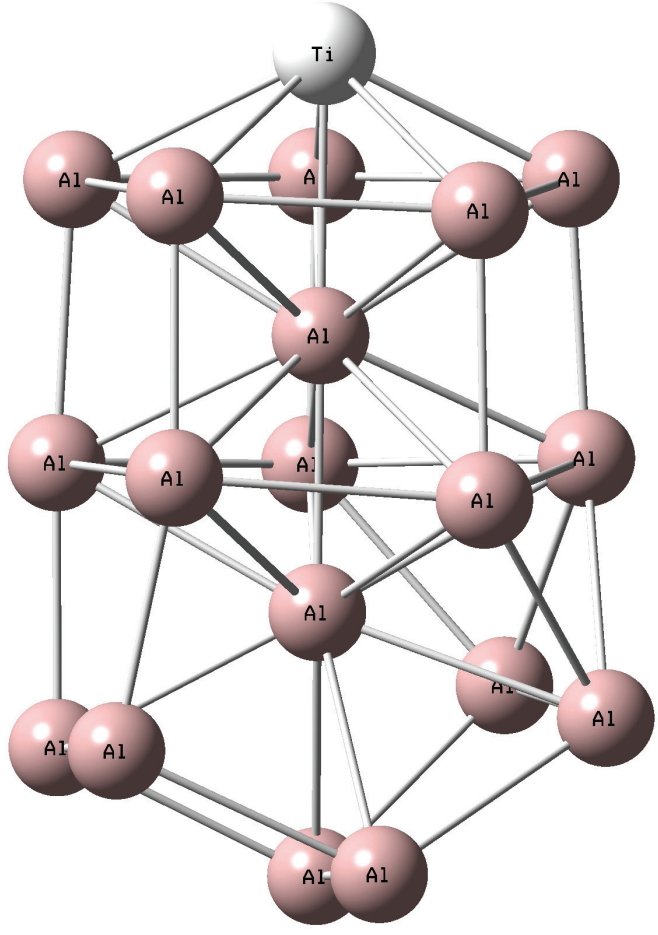

Figure 3. Geometrical structure of the most stable isomer of $Al_{18}Ti$ cluster

3.2. Electronic structure of the Al_{19}^+ and $Al_{18}Ti$ cluster

According to the shell model, or Jellium model, when forming a metal cluster, each metal atom will contribute its electrons, usually valence electrons, to the pool of shared electrons of the cluster. These shared electrons are filled into the molecular orbitals of the cluster, which are formed from linear combinations of the constituent atomic orbitals. The molecular orbitals containing these shared electrons are denoted as 1S, 1P, 1D, 2S, 2P, 2D, 1F,... (shell orbital). The shapes of these S, P, D, and F orbitals are similar to the shapes of the s, p, d, and f orbitals of atoms. The energy order of the shell orbitals of clusters according to the shell model (or Jellium model) is usually 1S, 1P, 1D, 2S, 2P, 2D, 1F, ...

3.2.1. Cluster Al_{19}^{+}

Each Al atom contributes 3 valence electrons to the common electron shell of the Al_{19}^{+} cluster. The number of valence electrons of the cluster is 56, and the electron configuration of the cluster is proposed as $1S^21P^62S^21D^{10}1F^{14}2P^62D^{10}2F^6$.

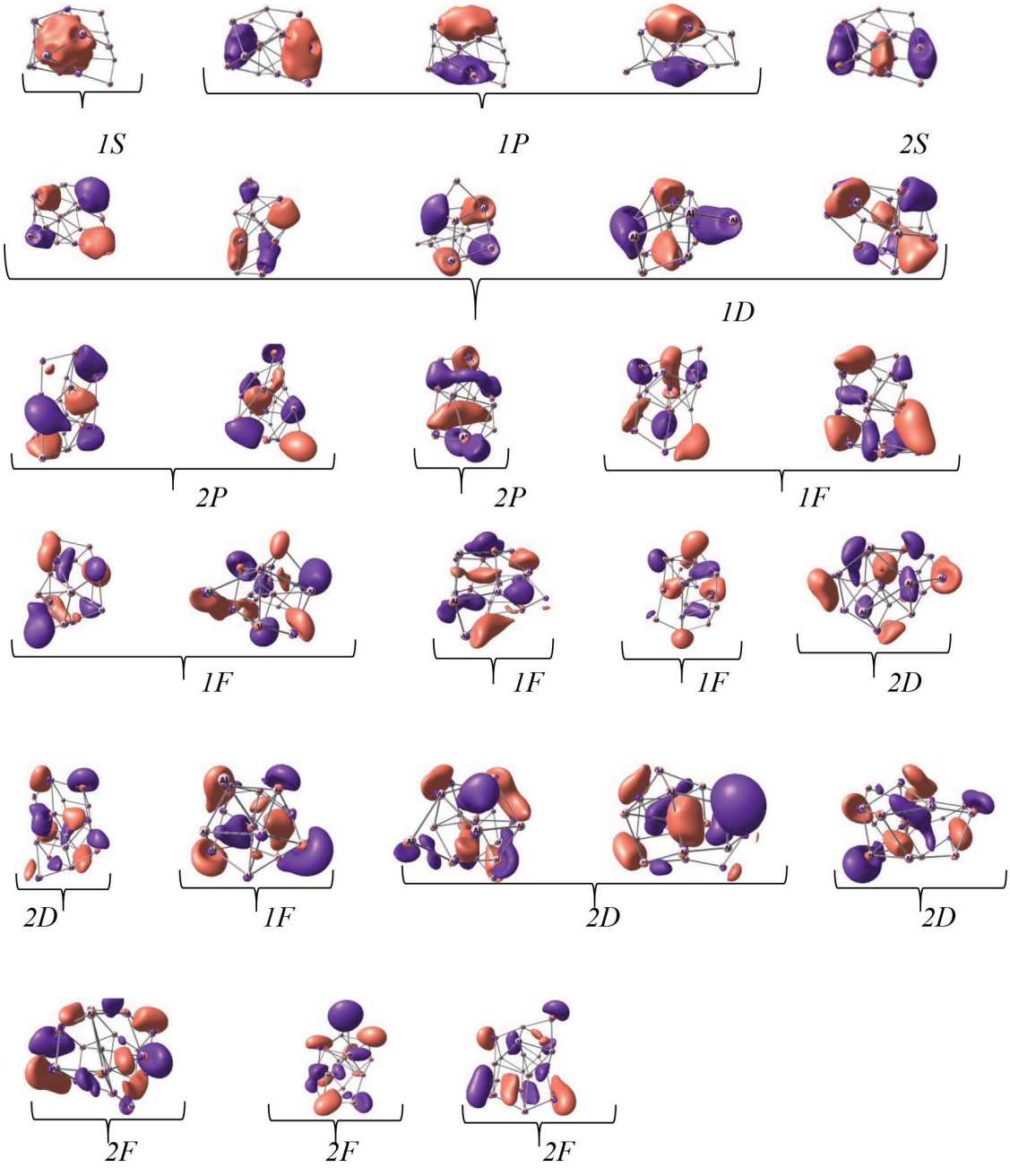

Figure 4. Shell orbitals 1S, 1P, 2S, 1D, 2P, 1F, 2D, 2F of the Al_{19}^{+} cluster.

After using Gauview software to draw images of MOs from the .fchk file created from the geometry optimization calculation, we found the MOs corresponding to the electron subshells of the Al_{19}^{+} cluster as shown in Figure 4. Thus, the MOs are not strictly distributed in the order as proposed. Specifically, we saw a separation of energy levels between MO 1P and MO 1D and the intervening existence of MO 2S in between the two subshells. In addition, between the MO 1F, we saw the appearance of MO 2P. Besides, the MO 2D and 2F also did not fill electrons in the order of the sub-shell proposed above.

3.2.2. Cluster $Al_{18}Ti$

The total number of valence electrons in the cluster is 58.

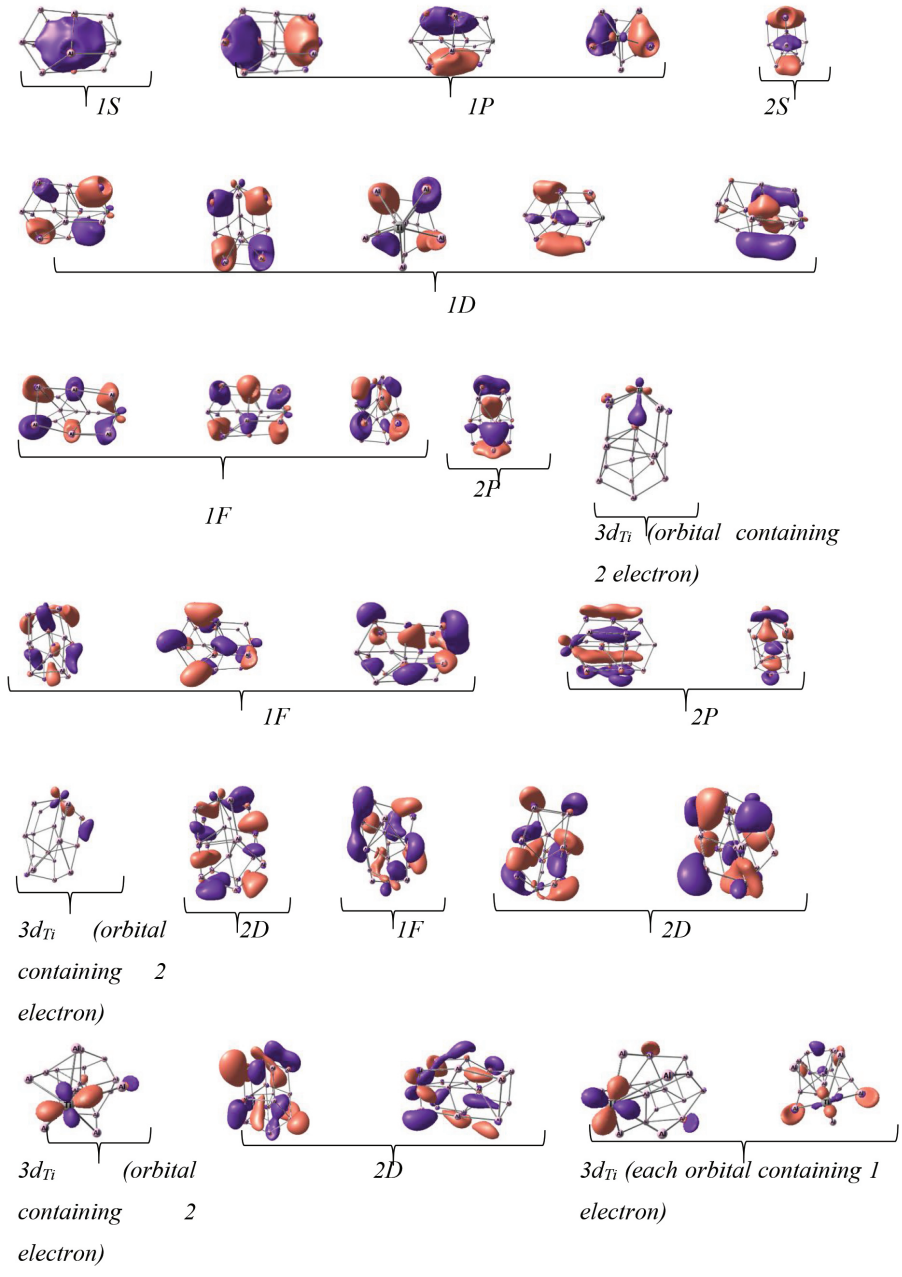

Figure 5. Shell orbital 1S, 1P, 2S, 1D, 2P, 1F, 2D, and 3d(Ti) of the cluster $Al_{18}Ti$ with spin multiplicity of 3

We found the MOs corresponding to the sub-shells of the most stable isomer of the $Al_{18}Ti$ cluster with a spin multiplicity of 3, as shown in Figure 5. Thus, the 58 shared electrons are distributed in the shell orbitals as well as the *3d* orbital of Ti order as predicted. The electron configuration is $1S^21P^62S^21D^{10}1F^62P^2 3d_{Ti}^{\ 2}1F^62P^4 3d_{Ti}^{\ 2}2D^21F^22D^4 3d_{Ti}^{\ 2}2D^4 3d_{Ti}^{\ 1} 3d_{Ti}^{\ 1}$.

In addition, we see the appearance of the structures of AO *3d* of the Ti atom, proving that the Ti atom has not contributed all 4 of its valence electrons to the cluster and has two unpaired electrons.

3.3. Investigation of catalytic activity of $Al_{18}Ti$ cluster for CO conversion reaction

The reaction $2CO + O_2 \rightarrow 2CO_2$ is highly exothermic with a negative Gibbs energy, indicating that the reaction is thermodynamically spontaneous. This means that the CO_2 product is more energetically stable than CO and O_2, and the reaction is likely to occur spontaneously when the conditions are right.

Although this reaction is thermodynamically spontaneous, it is kinetically very slow at room temperature. This is because the bonds in the O_2 molecule are strong double bonds (sigma bonds and pi bonds) with high bond energies, and CO also has a powerful triple bond between C and O. Therefore, the activation energy for this reaction is very high.

A catalyst can lower the activation energy by providing a surface on which CO and O_2 can adsorb, thereby weakening the initial bonds in the CO and O_2 molecules. This makes the reaction easier and faster. In practice, platinum (Pt) is often used as a catalyst for this reaction due to its good adsorption capacity for both CO and O_2.

The $Al_{18}Ti$ cluster system was chosen as a catalyst. Through the investigation of the geometric structure and electron structure of the $Al_{18}Ti$ cluster, we found that it is a stable cluster that still retains the double icosahedron symmetry of the Al_{19}^+ cluster, and the electron structure of the valence shell follows the Jellium model. In addition, the $Al_{18}Ti$ cluster system has the most stable isomer corresponding to the Ti atom replacing Al at the top apex of the double icosahedron, with a spin multiplicity of 3, corresponding to 2 unpaired electrons on the *3d* orbitals of Ti. Such geometrical and electron structures of the $Al_{18}Ti$ cluster will help this cluster catalyze the CO conversion process smoothly.

The CO conversion reaction with O_2 under the action of the $Al_{18}Ti$ catalyst can be divided into the following stages. The $Al_{18}Ti$ cluster accepts an O_2 molecule to form $Al_{18}TiO_{2;}$ the $Al_{18}TiO_2$ cluster accepts one CO molecule to form an $Al_{18}TiO_2$. CO cluster and converts to $Al_{18}TiO$. CO_2 and then desorbs a CO_2 molecule, forming an $Al_{18}TiO$ cluster. In the next stage, this cluster accepts another CO molecule, forming an $Al_{18}TiO$.CO cluster system and then converting to $Al_{18}Ti$. CO_2. This system finally desorbs the CO_2 molecule and regenerates the original catalyst cluster, $Al_{18}Ti$. These stages can be summarized into the following two main stages.

3.3.1. Stage 1. Formation and transformation of $Al_{18}TiO_2$.CO cluster

a. Geometrical and electron structures

The CO conversion investigation process was started from the stable structure of $Al_{18}Ti$, and then this cluster was allowed to receive O_2 and the structure of the new cluster was optimized to obtain the $Al_{18}TiO_2$ cluster (Figure 6).

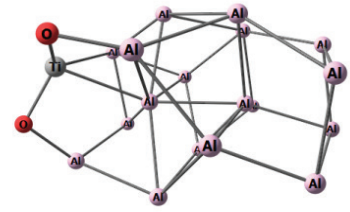

Figure 6. Geometrical structure of the $Al_{18}TiO_2$ cluster

The average bond lengths of the reactants ($Al_{18}Ti$ and O_2) and the intermediate $Al_{18}TiO_2$ are shown in Table 1.

Table 1. The bond lengths in the reactants and the intermediate $Al_{18}TiO_2$

Compound	$Al_{18}Ti$	O-O	$Al_{18}TiO_2$		
	Ti-Al	O-O	Ti-O	Ti-Al	O-O
Bond length (*Å*)	2.67	1.21	1.80	2.80	3.07

From the data in Table 1, it can be seen that after receiving O_2, the average bond length between Ti-Al increased by 0.13 Å, the average bond length between O-O increased by 1.86 Å. This proves that the O=O bond in molecular oxygen has been dissociated on the surface of the cluster.

Corresponding to the above geometrical structure, we find and attribute the electron structure of $Al_{18}TiO_2$ as shown in Figure 7. We only focus on assigning the AOs and MOs related to Ti and two O atoms.

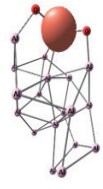

non-bonding AO *s* of Ti

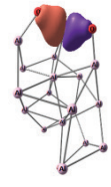

AO *p* of Ti bonding with O

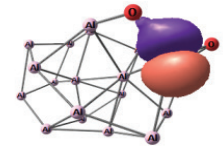

non-bonding AO *p* of Ti

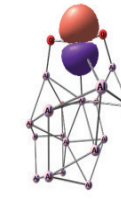

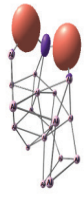

AO *s* of O

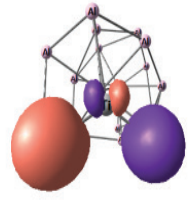

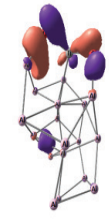

Bonding MO between Ti and O

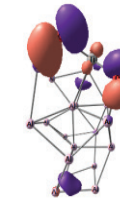

Bonding MO between O and Al

Figure 7. Electron structure of $Al_{18}TiO_2$

In this electron structure, Ti is the active site interacting with O_2. The position of Ti at the apex of the double icosahedron, along with its two unpaired electrons in the AO*3d,* facilitates the overlap between its *3d* orbitals with other orbitals, helping to weaken the O=O double bonds in the absorbed O_2 molecule.

The next step is the addition of one CO molecule via the C-end to the active site of the most stable structure of $Al_{18}TiO_2$, then performing the geometrical optimization of the system. The structure of $Al_{18}TiO_2$.CO is shown in Figure 8.

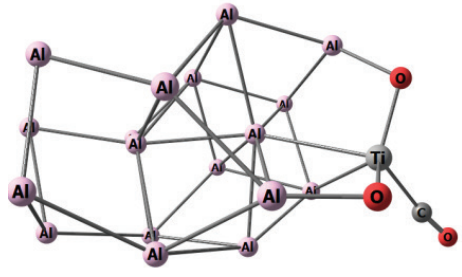

Figure 8. Geometrical structure of $Al_{18}TiO_2$.CO

The Ti-O, Ti-C bond lengths and the distance between one of the two O atoms and the C atom in the $Al_{18}TiO_2$.CO are 1.81, 2.14 and 3.29 Å, respectively.

Thus, based on the CO-O distance and the bonds formed between O atoms and Ti in the cluster, it can be predicted that the OTiC angular deformation vibration will help the CO molecule approach the O atom on the $Al_{18}Ti$ surface to react and form the CO_2 molecule.

The electron structure of the $Al_{18}TiO_2$.CO cluster was also investigated, and the results are shown in Figure 9.

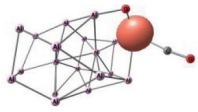

Non-bonding AO *s* of Ti

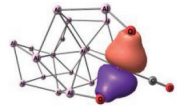

AOs *p* of Ti bonding with O

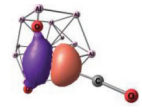

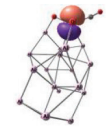

non-bonding AO *p* of Ti

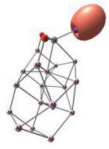

σ-bonding MO of CO

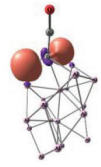

AOs *s* of O atoms

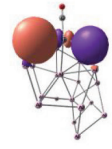

AOs *s* of O atoms

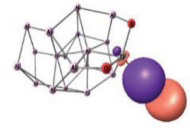

σ*-anti bonding MO of CO

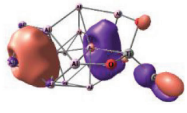

1P shell MO

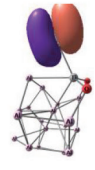

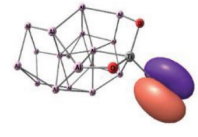

π-bonding MOs of CO

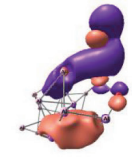

σ-bonding MO between Ti and CO

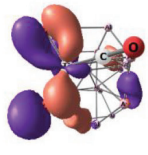

Bonding MO between Ti and O

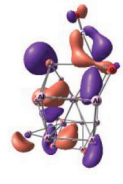

π-back donation MO between AO d of Ti and MO π* of CO

Figure 9. Electron structure of $Al_{18}TiO_2$.CO

The overlap between the *2p* orbital of carbon and the *3d* orbital of titanium creates a strong σ(Ti-C) bond. In addition, the overlap between the 3*d* orbitals of Ti and the empty π* anti-bonding orbital of CO will help to strengthen the bond between Ti and CO, while weakening the C≡O triple bond in the CO molecule. This is consistent with the model of σ-donation and π-back donation between the CO molecule and the transition metal in the carbonyl complex.

In the next step, the CO molecule approaches one of the two O atoms, forming CO_2, and the system is denoted as $Al_{18}TiO.CO_2$, see Figure 10.

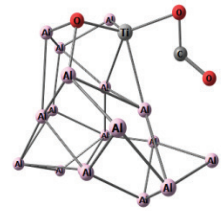

Figure 10. Geometrical structure of $Al_{18}TiO.CO_2$

The Ti-O, Ti-C bond lengths and the distance between one of the two O atoms and the C atom in the $Al_{18}TiO.CO_2$ are 1.97, 2.12 and 1.28 Å, respectively. It can be seen that for the $Al_{18}TiO.CO_2$ system, as compared with $Al_{18}TiO_2.CO$, the bond between Ti-O is elongated while the bond length between CO and O is shortened.

b. Bond orders

By using the natural bond orbital method NBO, we obtained the bond order value between Ti and the O and C elements, according to the Wiberg bond index shown in Table 2.

Table 2. The Wiberg bond index in the investigated compounds

Compound	Bond	Wiberg bond index
$Al_{18}TiO_2$	$Ti-O^{20}$	1.02
	$Ti-O^{21}$	0.99
$Al_{18}TiO_2.CO$	$Ti-O^{20}$	1.10
	$Ti-O^{21}$	1.04
	Ti-C	0.87
	$C-O^{23}$	2.16
$Al_{18}TiO.CO_2$	$Ti-O^{20}$	0.72
	$Ti-O^{21}$	0.65
	$C-O^{21}$	1.20
	$C-O^{23}$	1.66

The results showed that during the transformation from $Al_{18}TiO_2$ to $Al_{18}TiO_2$.CO, the bond order between Ti and O does not change. However, as the $Al_{18}TiO.CO_2$ formation occurred, both the bond orders between Ti-O and C-O decreased significantly, from which it can be predicted that the bonds between Ti-O and C-O are weakened, facilitating the formation of CO_2 from the cluster.

3.3.2. Stage 2: Formation and transformation of $Al_{18}TiO.CO$ cluster system

a. Geometrical structure and bonding order of the $Al_{18}TiO.CO$ cluster system

During the optimization of the possible structures formed in the second stage, we obtained two compounds, namely $Al_{18}TiO.CO$ and $Al_{18}Ti.CO_2$, whose structures are shown in Figure 11.

(a) (b)

Figure 11. The cluster Al18Ti attached by CO (a) and CO2 (b)

The Ti-O, Ti-C, and CO bond lengths and bond orders in the two clusters are listed in Table 3.

Table 3. The Ti-O, Ti-C, and CO bond lengths and orders in the $Al_{18}TiO.CO$ and $Al_{18}Ti.CO_2$ clusters

Compound	$Al_{18}TiO.CO$		$Al_{18}Ti.CO_2$		
Bond		Ti-C	$Ti-O^{20}$	$C-O^{20}$	$C-O^{22}$
$Ti-O^{20}$					
Bond length (Å)	1.80	2.13	1.97	1.26	1.26
Bond order	1.09	0.90	0.61	1.22	1.63

From results in Table 3, we can see that the bond order between Ti-O in $Al_{18}Ti.CO_2$ is reduced compared to that in $Al_{18}TiO.CO$, while the CO bond length and order in $Al_{18}Ti.CO_2$ are close to those in the CO_2 molecule. Based on the bond lengths and orders, it can be predicted that the CO_2 is formed in the $Al_{18}Ti.CO_2$ cluster system.

b. Electron structure of the $Al_{18}TiO.CO$ cluster system

The electron structure of the $Al_{18}TiO.CO$ is characterized by the MOs that are shown in Figure 12. For this cluster, the σ bonding orbital and σ^* anti-bonding orbital of CO are clearly shown, and two π bonds of CO can be fully attributed.

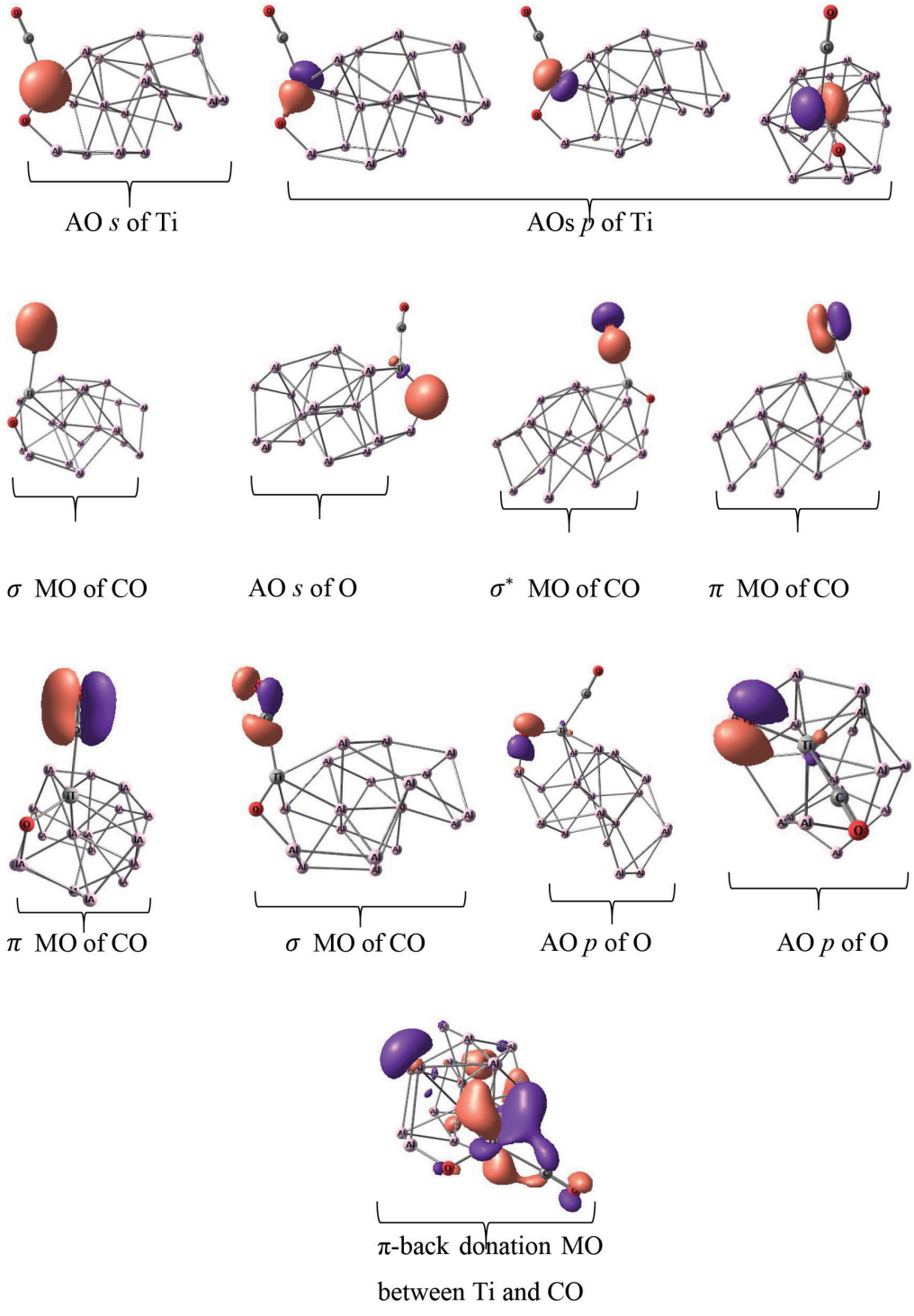

Figure 12. Electron structure of $Al_{18}TiO.CO$

For the cluster $Al_{18}Ti.CO_2$, the MO representing the formation of CO_2 is shown in Figure 13.

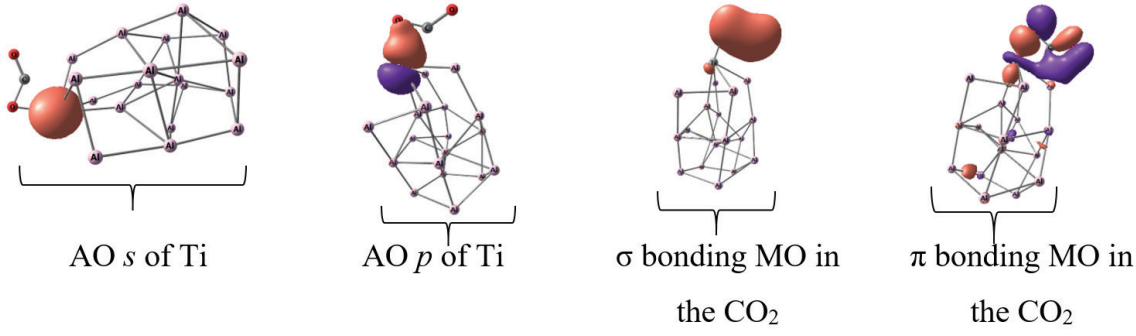

Figure 13. Electron structure of $Al_{18}Ti.CO_2$

c. Vibration frequency of CO in the cluster system

The addition of CO onto the surface of the $Al_{18}Ti$ cluster affects the vibrational frequency of CO. Specifically, the calculated stretching vibrational frequency of CO appears around 2212 cm^{-1} in the infrared spectrum, which is larger than the experimental value of 2143 cm^{-1}. This band is very intense and sharp due to the much greater change in dipole moment during the vibration. However, after being absorbed by the $Al_{18}Ti$ cluster, although the pattern is still intense and sharp, the calculated vibrational frequency of CO decreases to 2015 cm^{-1}. Thus, it can be concluded that the CO coordination with Ti has weakened the bond between C and O.

4. CONCLUSION

The geometrical and electron structures of the Al_{19}^+ and $Al_{18}Ti$ clusters were studied by the DFT method using the B3LYP functional and the 6-311+G(d) basis set. The clusters adopt the double icosahedron structure, and the Ti replaces the Al atom at the top apex of the double icosahedron in the case of the $Al_{18}Ti$ cluster. There is energy level splitting of the 1P, 1D, 1F, 2P, and 2D shell orbitals due to the double icosahedral structure of the cluster, and the *3d* orbitals of the Ti transition metal change the electron properties of the cluster. The catalytic activity of the $Al_{18}Ti$ cluster for the CO oxidation has been investigated initially. The Ti atom in $Al_{18}Ti$ (spin multiplicity of 3) plays a central role in binding to CO and O_2. When Ti coordinates with O_2 it breaks the O=O bond, then it coordinates with CO and weakens the C≡O triple bond, facilitating CO to approach the O atom and form CO_2.

Acknowledgment: The authors would like to thank the Center for Computational Science, Hanoi National University of Education, for the computational facilities.

Author Information:

Pham Thi Thanh Hoa, Faculty of Chemistry, Hanoi National University of Education - Center for Computational Science, Hanoi National University of Education, Vietnam

Dr. Ngo Tuan Cuong, *(*Corresponding author),* Faculty of Chemistry, Hanoi National University of Education—Center for Computational Science, Hanoi National University of Education, Vietnam

Email: cuongnt@hnue.edu.vn

Article Information

Received: November 7, 2024

Revised: December 9, 2024

Accepted: December 10, 2024

Note

The authors declare no competing interests.

5. REFERENCES

Baletto, F., & Ferrando, R. (2005). Structural properties of nanoclusters: Energetic, thermodynamic, and kinetic effects. *Reviews of Modern Physics, 77*(371), p. 5156.

Becke, A. D. (1993). Density-functional thermochemistry. III. The role of exact exchange, *J. Chem. Phys., 98,* p. 5648.

Charkin, O. P., Charkin, D. O., Klimenko, N. M., & Mebel, A. M. (2002). A theoretical study of isomerism in doped aluminum XAl_{12} clusters (X = B, Al, Ga, C, Si, Ge) with 40 valence electrons. *Chemical Physics Letters, 365,* p. 494.

Chen, M., Zhang, L., & Wu, X. (2021). Electronic structure and properties of aluminum clusters: A computational study. *Computational Materials Science, 182,* p. 109763.

Chuang, F. C., Wang, C., & Ho, K. (2006). Structure of neutral aluminum clusters Al_n ($2 \leqslant n \leqslant 23$): Genetic algorithm tight-binding calculations. *Physical Review B, 73,* p. 125431.

Esquivel, J., & Gupta, R. K. (2017). Corrosion behavior and hardness of Al–M (M: Mo, Si, Ti, Cr) alloys. *Acta Metallurgica Sinica, 30,* p. 333.

Fan, B., Ge, G. X., Jiang, C. H., Wang, G. H., & Wan, J. G. (2017). Structure and magnetic properties of icosahedral Pd_xAg_{13-x} (x = 0–13) clusters. *Scientific Reports, 7* (1).

Frisch, M. J., Schlegel, H. B., Scuseria, G. E., Robb, M. A., Cheeseman, J. R. & Montgomery, J. A. (2009). *Gaussian 09 Revision: D.01*.

Ge, G. X., Han, Y., Wan, J. G., Zhao, J. J., & Wang, G. H. (2013). The role of TM's (M's) d valence electrons in $TM@X_{12}$ and $M@X_{12}$ clusters. *Journal of Chemical Physics, 139,* p. 174309.

Hohenberg, P. & Kohn, W. (1964). Inhomogeneous Electron Gas, *Phys. Rev. B, 136*, 864.

Jia, J., Wang, J. Z., Liu, X., Xue, Q. K., Li, Z. Q., Kawazoe, Y., & Zhang, S. B. (2002). Artificial nanocluster crystal: Lattice of identical Al clusters. *Applied Physics Letters, 80,* p. 3186.

Knickelbein, M. B. (2001). Experimental observation of superparamagnetism in manganese clusters. *Physical Review Letters, 86,* p. 5255.

Li, H. F., Kuang, X. Y., & Wang, H. Q. (2011). Probing the structural and electronic properties of lanthanide-metal-doped silicon clusters: $M@Si_6$ (M = Pr, Gd, Ho). *Physics Letters A, 375,* p. 2836.

Li, X., Kuznetsov, A. E., Zhang, H. F., Boldyrev, A. I., & Wang, L. S. (2001). Observation of all-metal aromatic molecules. *Science, 291,* p. 859.

Li, X., Zhang, H., Wang, L., Kuznetsov, A. E., Cannon, N. A., & Boldyrev, A. I. (2001). Experimental and theoretical observations of aromaticity in heterocyclic XAl_3^- (X = Si, Ge, Sn, Pb) systems. *Angewandte Chemie, 113,* p. 1919.

Li, Y., Tam, N. M., Woodham, A. P., Lyon, J. T., Li, Z., Lievens, P., Fielicke, A., Nguyen, M. T., & Janssens, E. (2016). Structural evolution and electronic properties of $CoSi_n^-$ (n = 3-12) clusters: Mass-selected anion photoelectron spectroscopy and quantum chemistry calculations. *Journal of Physical Chemistry C, 120,* p. 19454.

McLean, A. D. & Chandler, G. S. (1980). Contracted Gaussian-basis sets for molecular calculations. 1. 2nd row atoms, Z=11-18, *J. Chem. Phys., 72,* p.p. 5639-48.

Nguyen Minh Tam, Long Van Duong, Ngo Tuan Cuong, & Minh Tho Nguyen (2019). Structure, stability, absorption spectra and aromaticity of the singly and doubly silicon doped aluminum clusters $Al_nSi_m^{0/+}$ with n = 3-16 and m = 1, 2†. *RSC Adv., 9,* p. 27208.

Perdew, J. P., Burke, K. & Ernzerhof, M. (1996). Generalized gradient approximation made simple, *Phys. Rev. Lett., 77*, p. 3865.

Raghavachari, K., Binkley, J. S., Seeger, R. & Pople, J. A. (1980). Self-Consistent Molecular Orbital Methods. 20. Basis set for correlated wave-functions, *J. Chem. Phys., 72,* p.p. 650-54.

Rao, B. K., & Jena, P. (1999). Evolution of the electronic structure and properties of neutral and charged aluminum clusters: A comprehensive analysis. *Journal of Chemical Physics, 111,* p. 1890.

Reinhard, P. G., & Suraud, E. (2004). *Introduction to Cluster Dynamics*. Wiley-VCH.

Roach, P. J., Woodward, W. H., Castleman, A. W., Reber, A. C., & Khanna, S. N. (2009). Active sites, spin, and reactivity of clusters. *Science, 323,* p. 492.

Sengupta, T., Das, S., & Pal, S. (2016). Transition metal doped aluminum clusters: An account of spin. *Journal of Physical Chemistry C, 120,* p. 10027.

Wang, M., Huang, X., Du, Z., & Li, Y. (2009). Structural, electronic, and magnetic properties of a series of aluminum clusters doped with various transition metals. *Chemical Physics Letters, 480*, p. 258.

Wang, Y., & Li, Y. (2020). Computational studies on the electronic structure of aluminum clusters with various dopants. *Journal of Molecular Modeling, 26,* p. 50.

Varano, A., Henry, D. J., & Yarovsky, I. (2010). Theoretical study of the geometries and dissociation energies of molecular water on neutral aluminum clusters Al_n (n = 2–25). *Journal of Physical Chemistry A, 114,* p. 3602.

Wang, H. Q., Kuang, X. Y., & Li, H. F. (2010). Density functional study of structural and electronic properties of bimetallic copper–gold clusters: Comparison with pure and doped gold clusters. *Physical Chemistry Chemical Physics, 12,* p. 5156.

Yang, J. M., Zhao, T., Ge, G. X., & Zhang, X. (2016). Manipulation of magnetic anisotropy in Irn+1 clusters by Co atom. *Physica A: Statistical Mechanics and its Applications, 453,* p. 194.

NGHIÊN CỨU BẰNG LÝ THUYẾT PHIẾM HÀM MẬT ĐỘ VỀ CẤU TRÚC HÌNH HỌC VÀ CẤU TRÚC ĐIỆN TỬ CỦA CÁC CỤM NGUYÊN TỬ $Al_{18}Ti$ VÀ HOẠT ĐỘNG XÚC TÁC CỦA CHÚNG ĐỐI VỚI QUÁ TRÌNH OXY HÓA CO

Phạm Thị Thanh Hoa[1,2], Ngô Tuấn Cường[1,2,*]

[1]Khoa Hóa học, Đại học Sư phạm Hà Nội, Việt Nam

[2]Trung tâm Khoa học tính toán, Đại học Sư phạm Hà Nội, Việt Nam

Tóm tắt: *Phiếm hàm B3LYP kết hợp với bộ cơ sở 6-311+G(d) đã được sử dụng để tối ưu hóa các cấu trúc hình học cùng với tần số dao động của các cụm nguyên tử Al_{19}^+ và $Al_{18}Ti$ hội tụ về cấu trúc nhị thập diện kép, và các vị trí Ti ở đỉnh trên cùng của hình nhị thập diện kép trong trường hợp cụm $Al_{18}Ti$. Những thay đổi trong cấu trúc electron của các cụm đã được xác định, theo đó có sự phân tách mức năng lượng của các orbital lớp 1P, 1D, 1F, 2P, 2D và sự xuất hiện của các orbital 3d của Ti trong cấu hình electron. Khả năng xúc tác của cụm $Al_{18}Ti$ đối với phản ứng CO và O_2 đã được nghiên cứu sơ bộ, nguyên tử Ti đóng vai trò trung tâm trong việc liên kết với CO và O_2, làm suy yếu cả liên kết O=O và C≡O và tạo điều kiện cho sự hình thành CO_2.*

Keywords: *Al_{19}^+, cụm $Al_{18}Ti$, lý thuyết phiếm hàm mật độ (DFT), lý thuyết phiếm hàm mật độ phụ thuộc thời gian (TD-DFT), quá trình oxy hóa CO*

*** Thông tin tác giả:**

Phạm Thị Thanh Hoa, Khoa Hóa học, Đại học Sư phạm Hà Nội, Việt Nam - Trung tâm Khoa học tính toán, Đại học Sư phạm Hà Nội, Việt Nam

TS. Ngô Tuấn Cường *(*Tác giả liên hệ)*, Khoa Hóa học, Đại học Sư phạm Hà Nội, Việt Nam - Trung tâm Khoa học tính toán, Đại học Sư phạm Hà Nội, Việt Nam

Email: cuongnt@hnue.edu.vn

Ghi chú

Các tác giả đã xác nhận không có tranh chấp về lợi ích đối với bài báo này.